Proc. Natl. Acad. Sci. USA
Vol. 91, pp. 5813–5817, June 1994
Biochemistry

GTP-dependent polymerization of *Escherichia coli* FtsZ protein to form tubules

(cytokinesis/septum synthesis/cytoskeleton/tubulin-like/microtubule)

DAVID BRAMHILL AND CHRIS M. THOMPSON

Department of Enzymology, Building 80Y-325, Merck Research Laboratories, P.O. Box 2000, Rahway, NJ 07065–0900

Communicated by Edward M. Scolnick, March 21, 1994

ABSTRACT **The FtsZ protein is a GTPase that is essential for cell division in *Escherichia coli*. During cytokinesis, FtsZ localizes to a ring at the leading edge of septum synthesis. We report the GTP-dependent polymerization of purified FtsZ measured by sedimentation and light scattering. Electron microscopy of polymerized FtsZ revealed structures including tubules 14–20 nm in diameter with longitudinal arrays of protofilaments. FtsZ depolymerized upon removal of GTP and repolymerized after subsequent GTP addition. Mutant FtsZ84 protein polymerized inefficiently, suggesting that polymerization is important for the cellular role of FtsZ in division. The possibility that tubules of FtsZ protein form a cytoskeleton involved in septum synthesis is consistent with our data.**

Cell division in rod-shaped bacteria is accomplished by synthesis of a septum across the middle of the cell (1, 2). Genetic studies have identified numerous genes required for septum synthesis (cytokinesis) in *Escherichia coli* (3). The protein encoded by *ftsZ* is essential for cell division (4–6) and is one of the earliest acting septum synthesis factors (7, 8). The FtsZ protein is highly conserved among diverse eubacteria (9–12). It appears to be the target of several cellular division inhibitors, including the SOS-induced SulA protein (13, 14) and MinC-MinD proteins involved in selection of the division site (15–17).

Immediately before cytokinesis begins, FtsZ relocalizes from the cytoplasm to a ring at the inner membrane at the midpoint of the cell. As the cell invaginates, FtsZ remains in a diminishing ring at the leading edge of septum synthesis until division is completed, whereupon it redistributes to the cytoplasm (18). The FtsZ protein has been purified and shown to be a GTPase, an activity essential for its function (19–21). Sequence alignments indicate limited homology with tubulins (19, 20), tempting speculation that FtsZ may be a structural protein. However, alternative explanations are also consistent with the cellular localization and GTPase of FtsZ. FtsZ might serve as a multimeric guanine nucleotide binding protein switch to trigger assembly of the septum synthesis machinery (21) or as a motor protein to provide the force for invagination of the cell wall and membrane. To distinguish between these models, the properties of purified FtsZ were further characterized.

We report here biochemical and electron microscopic evidence demonstrating the GTP-dependent polymerization of wild-type FtsZ protein and that a mutant FtsZ protein polymerizes inefficiently. Our data support the notion that FtsZ may be a major component of a bacterial cytoskeleton involved in septum synthesis.

MATERIALS AND METHODS

Reagents. Chemicals were purchased from Sigma unless stated otherwise. Nucleotides were obtained from Boehringer Mannheim. Restriction enzymes and T4 DNA ligase were purchased from New England Biolabs. Carbon-coated copper grids and reagents for electron microscopy were from Ted Pella (Redding, CA).

Plasmid Constructions. The wild-type *ftsZ* coding sequence was amplified by polymerase chain reaction methodology and cloned between the *Nde* I and *Bam*HI sites of the vector pET11a (Novagen) to give plasmid pET11-FtsZ. Site-directed mutagenesis of the gene was used to derive the *ftsZ84* mutant plasmid pET11-FtsZ84. The sequence of each allele was confirmed (Julia Hsu, C.M.T., and D.B., unpublished data).

Purification of FtsZ Proteins. *E. coli* BL21 (DE3)/pLysS transformed with the appropriate plasmid was used to overexpress each FtsZ protein. Wild-type FtsZ and FtsZ84 proteins were purified essentially as described (21).

Polymerization Assays. Standard reaction mixtures (200 μl) contained 1 mg of FtsZ per ml in POL buffer [40 mM Tris·HCl, pH 7.5/5 mM magnesium acetate/40 mM potassium glutamate/8% (vol/vol) glycerol/0.08% Triton X-100]. Where indicated, nucleotide was added to 5 mM. After incubation at 37°C for 30 min, centrifugation was at 100,000 rpm in a Beckman TLA100.1 rotor at 37°C for 30 min. Supernatants were decanted and pellets were resuspended in a starting volume (200 μl) of POL buffer lacking magnesium. Protein was determined with Bio-Rad protein assay reagent. Actin was cycle purified from rabbit muscle acetone powder (22).

RESULTS

The dynamic distribution of FtsZ protein during the cell cycle (18) and the similarities with tubulins in sequence and in GTP binding (19–21) point to a possible structural role. We tested whether, like tubulin, FtsZ might polymerize in the presence of GTP (23). Indeed, purified FtsZ supplemented with magnesium became gel-like and opalescent within 10 sec of GTP addition, suggesting that polymerization had occurred. Several independent methods were used to confirm this initial observation.

GTP-Dependent Sedimentation. Polymerized tubulin and actin sediment rapidly during ultracentrifugation (22, 24). In the presence of GTP, almost all of the FtsZ protein was recovered in the pellet (Fig. 1). An internal control, bovine serum albumin, remained in the supernatant. Little FtsZ protein sedimented without GTP or when ATP replaced GTP. Over 65% of total FtsZ was sedimented by 2 min of centrifugation, compared with 40% of a polymerized actin control, indicating that FtsZ forms massive multimers in the presence of GTP.

GTP-Dependent Light Scattering. A second assay, based on light scattering by large molecular assemblies (25), was used. Without GTP, FtsZ protein scattered little light at 340 nm. After GTP addition, a 27-fold increase in scattering was observed. Light scattered by FtsZ polymers was essentially unchanged in wavelength and polarization. Since scattering

The publication costs of this article were defrayed in part by page charge payment. This article must therefore be hereby marked "*advertisement*" in accordance with 18 U.S.C. §1734 solely to indicate this fact.

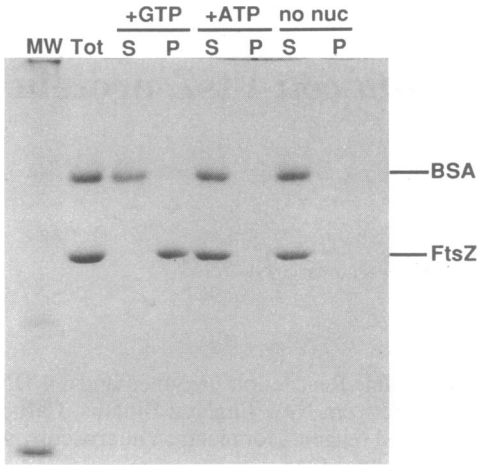

FIG. 1. Analysis on SDS/polyacrylamide gel of FtsZ complexes sedimented in the presence of various nucleotides. Reaction mixtures contained 1 mg FtsZ 25 per ml and 1 mg of bovine serum albumin (BSA) per ml (as an internal control) in 200 μl of POL buffer plus 5 mM nucleotide, as indicated. After ultracentrifugation, supernatants were decanted and pellets were redissolved in 200 μl. Aliquots of each sample in gel loading buffer were run on a SDS/12% polyacrylamide gel and stained with Coomassie blue. S, supernatant; P, pellet; MW, molecular weight standards; Tot, starting sample.

reduces the transmitted light, optical density at 340 nm could be measured more conveniently and quantitatively. The requirements for light scattering (A_{340}) and for sedimentation were identical (Table 1). Neither dGTP nor ATP could substitute for GTP. Magnesium was required. Similar specificity is reported for FtsZ GTPase (19–21). FtsZ can bind GDP and GTP[γS] (19–21); therefore, the inability of these nucleotides to promote polymerization suggests a requirement for GTP hydrolysis at some step in FtsZ assembly.

Rate of Polymerization. To confirm the rapid kinetics indicated by the initial observations of the changes in turbidity and viscosity, stopped-flow measurements were made. FtsZ exhibited a burst in polymerization followed by a second, slower phase (Fig. 2). The magnitude of the burst was proportional to the initial concentration, and the transition to slower kinetics occurred at ≈0.5 sec, independent of concentration. These observations could be explained by two populations of FtsZ in the initial solution, one of which is ready to polymerize rapidly and a second that polymerizes more slowly.

There is no evidence for a lag due to nucleation of FtsZ under these conditions. The rate-limiting step in FtsZ polymerization appears to be different from that for tubulin polymerization (25). The initial rate is also much more rapid for FtsZ than is reported for tubulin (25).

Table 1. Correlation of light scattering and sedimentation

Addition(s)	A_{340}	FtsZ pelleted, % of total
Mg	0.000	4
GTP	0.020	8
GTP + Mg	0.620	86
GDP + Mg	0.010	5
GTP[γS] + Mg	0.005	6
dGTP + Mg	0.000	7
ATP + Mg	0.025	5

FtsZ protein at 1 mg/ml was incubated in POL buffer with the indicated additions (final concentration, 5 mM). After 30 min, A_{340} was measured and the fraction of FtsZ sedimented by ultracentrifugation was determined.

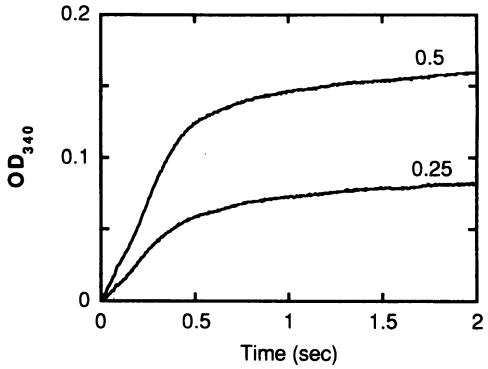

FIG. 2. Time course of FtsZ polymerization. Equal volumes of FtsZ in POL buffer and 10 mM GTP in POL buffer were mixed in an Applied Photo physics model DX.17MV sequential stopped-flow spectrophotometer to give the indicated final concentrations of FtsZ. A_{340} was recorded every 0.005 sec after mixing.

Polymerization was slower and less efficient at lower temperatures. However, polymers formed at 37°C sedimented with indistinguishable efficiency at 4°C and at 37°C.

FtsZ Forms Tubules. Direct observations of polymerized FtsZ suggest that it forms tubules. Samples of FtsZ were polymerized, adsorbed to carbon-coated grids, stained, and examined in the electron microscope (Fig. 3). The most abundant structures were tubule-like in appearance, although some variation in form was apparent. Tubules were up to 20 μm long, several times the length of a dividing cell. In 10 fields of FtsZ polymerized with GTP, >680 individual tubules could be counted. Control experiments lacking GTP showed no tubule structures in 10 equivalent fields, only a very few globular forms.

At high magnification, individual tubules of ≈15 nm diameter were seen with uranyl acetate and with phosphotungstic acid stains. Samples stained with uranyl acetate showed parallel striations along the tubule axis. In this regard, the FtsZ tubules resembled microtubules, which are typically composed of 13 tubulin protofilaments arranged superhelically (26–28). Several such protofilaments were visible in a tubule, spaced ≈3.5 nm apart in the structures in Fig. 3*A*. Individual FtsZ protofilaments seemed to have a beaded structure, with beads spaced approximately every 3.5 nm. Assuming that both tubulin and FtsZ molecules are approximately spherical, then a sphere of 3.5 nm for the 38-kDa FtsZ monomer would have a density virtually identical to a 4-nm sphere occupied by a 55-kDa tubulin monomer within a microtubule protofilament.

Sectioning was used to determine whether FtsZ forms hollow tubules. After polymerization, FtsZ was sedimented and the pelleted protein was fixed, embedded, sectioned, and stained. Oblique sections of parallel structures were abundant in the pellet (Fig. 3*C*). Interspersed among the regions of oblique and longitudinal sections, areas of transverse sections could also be seen. The transverse sections included structures that stained only around an outer ring and not in their center, appearing hollow. Like the longitudinal sections, the width of the staining was 4–5 nm. Fifty of the hollow sections were measured from the negatives. Their outer diameters varied from 14 to 20 nm, with a mean value of 16.8 nm, consistent with the size of the objects seen in Fig. 3 *A* and *B*. Similar, apparently hollow structures were seen in sections of FtsZ using other stains, including tannic acid, but no staining revealed the precise subunit architecture of the tubules. These observations suggest that a significant proportion of the polymer was in the form of hollow tubules with walls 4–5 nm thick. While this is close to what is expected for a tubule formed of a single layer of 3.5-nm-diameter protofilaments, no detail of subunit arrangements in these struc-

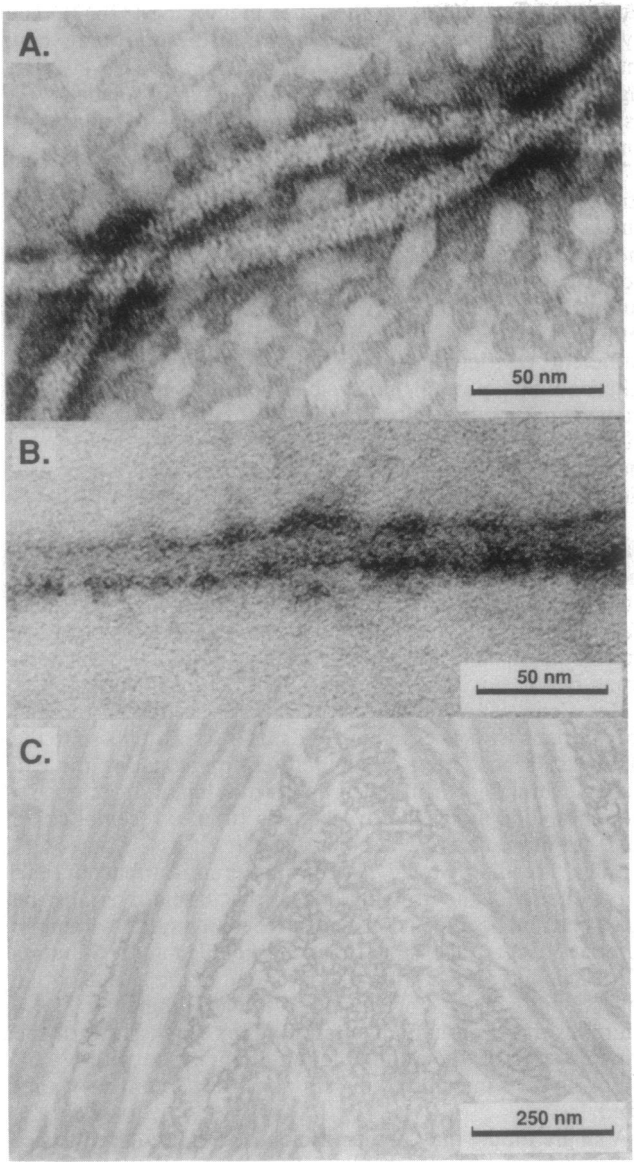

FIG. 3. Electron micrographs of polymerized FtsZ. (*A*) FtsZ at 20 μg/ml was polymerized in POL buffer plus 6 mM GTP for 15 min, spotted onto a carbon-coated grid for 30 sec, and then stained with 2% uranyl acetate for 45 sec. (*B*) As in *A* but stained with 1% phosphotungstate. (*C*) Thin section of sedimented FtsZ polymers. FtsZ at 1 mg/ml was polymerized in POL buffer with 6 mM GTP and sedimented. The pellet was fixed with 3% glutaraldehyde in 6 mM GTP-containing POL buffer at 4°C overnight, embedded in Epon, and sectioned before staining with 2% uranyl acetate for 10 min. Grids were examined with a Philips 300 electron microscope at 70 kV.

tures was visible with either uranyl acetate or phosphotungstic acid staining. Further studies will be required to define the exact subunit composition of the FtsZ tubules.

In addition to the tubules, other structures were visible. They were irregular in shape and size and might correspond to tubules broken during sedimentation, to incompletely formed tubules, or to an alternative form of FtsZ polymer, such as ribbons or sheets. These structures also had ≈4-nm-wide staining, suggesting a unit layer of FtsZ.

Polymerization Is Reversible. A common property of dynamic cytoskeletal proteins is that their polymerization is reversible (29). Tubulin and actin can be purified by cycles of polymerization–depolymerization (22, 24) (Fig. 4). Sedimented FtsZ depolymerized within 15 min when suspended

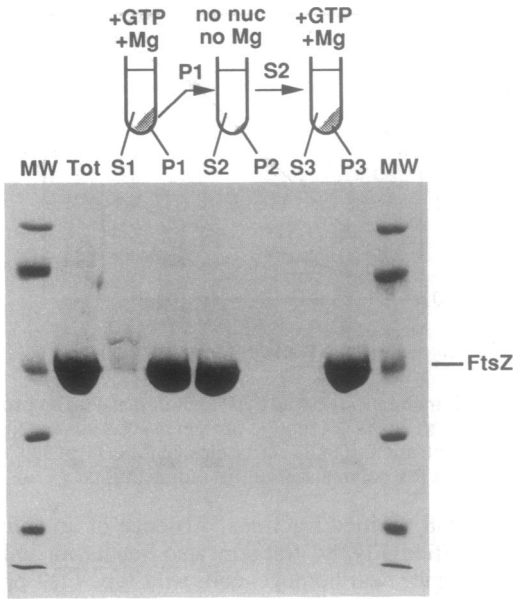

FIG. 4. SDS/polyacrylamide gel of the FtsZ protein after cycles of polymerization–depolymerization. FtsZ protein (200 μg in 200 μl) was polymerized with 6 mM GTP in POL buffer and sedimented; the pellet (P1) was redissolved in 200 μl of POL buffer lacking magnesium and GTP. The redissolved FtsZ was centrifuged again at 100,000 rpm, to give the supernatant (S2) and pellet (P2). To S2 was added 5 mM magnesium and 6 mM GTP before the sample was again centrifuged at 100,000 rpm, and the pellet (P3) was redissolved in 200 μl of POL buffer. Aliquots (2.5 μl) of each supernatant (S1–S3) and redissolved pellet (P1–P3) were analyzed on a SDS/12% polyacrylamide gel stained with Coomassie blue. The yield of FtsZ in the final pellet was 170 μg, representing 85% recovery of the starting sample (Tot). MW, molecular weight standards.

in buffer lacking both GTP and magnesium. This depolymerized FtsZ protein remained in the supernatant during subsequent centrifugation but was again sedimented when GTP and magnesium were added (Fig. 4). This cycling process removed trace contaminating proteins, strengthening the evidence that polymerization is intrinsic to FtsZ. Any putative auxiliary factor for polymerization of FtsZ represents <1% of cycle purified FtsZ (based on densitometry of a 10-μg sample of FtsZ run on SDS/polyacrylamide gel). For comparison, microtubule-associated proteins constitute up to 20% of tubulin purified by cycles of polymerization–depolymerization (30, 31).

While FtsZ remained polymerized when GTP was present, it depolymerized in the presence of GDP with similar efficiency as in the absence of nucleotide. This is consistent with the inability of GDP to support polymerization.

FtsZ84 Mutant Polymerizes Inefficiently. If the polymerization of FtsZ is involved in its normal function, then a loss of function mutant FtsZ protein might fail to polymerize. Cells bearing the mutant allele *ftsZ84* form long filaments at the restrictive temperature (32). It is likely that the defect in *ftsZ84* is only partial, since a modest increase in expression of the mutant protein can restore normal division activity (33). Using the plasmid pET11-FtsZ84 to direct high-level expression, the FtsZ84 mutant protein was purified to near homogeneity by the same procedure as for the wild-type protein.

Polymerization of FtsZ84 was only one-third that of wild type (Fig. 5). The defect in the mutant FtsZ84 protein was similar at 30°C and at 40°C both for polymerization and for GTPase activity (unpublished data). The reduced polymerization of purified FtsZ84 is unlikely to be due to contamination with an inhibitor, since wild-type protein polymerizes equally efficiently from the crude ammonium sulfate fraction

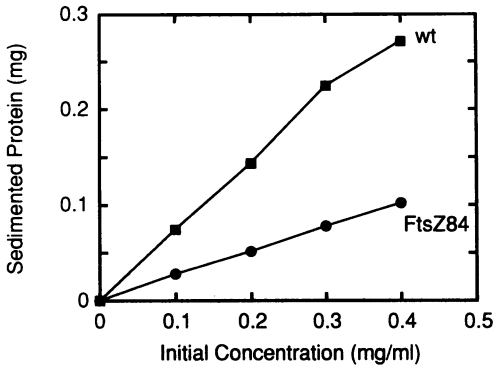

FIG. 5. Polymerization of wild-type and mutant FtsZ84 proteins. Wild-type FtsZ (■) or FtsZ84 mutant protein (●) was incubated at the indicated concentration in POL buffer plus 6 mM GTP at 37°C for 30 min and assayed for polymerization by sedimentation.

as from column purified fractions. Absence of an activator from the purified FtsZ84 fraction also seems an unlikely explanation, since near homogeneous wild-type FtsZ protein can polymerize very efficiently (see Fig. 4).

It should be noted that the critical concentration for both wild-type and mutant proteins appeared to be significantly below 0.1 mg/ml based on the near linear titrations observed.

DISCUSSION

The ability of wild-type FtsZ protein to polymerize in a GTP-dependent manner has been demonstrated by several independent methods. After addition of GTP, FtsZ solutions became gel-like, the FtsZ protein could be sedimented rapidly, and light scattering increased dramatically. Electron micrographs suggest that hollow tubules were formed by FtsZ, likely composed of parallel longitudinal arrays of FtsZ subunits. Assembly of FtsZ was reversible, allowing purification by cycles of polymerization–depolymerization. The ability to measure polymerization of purified FtsZ protein permits a molecular analysis of its role in cell division and its regulation by SulA (13, 14) and MinC-MinD proteins (15–17).

Significance of FtsZ Polymerization. Although tubules of FtsZ have not been observed in a dividing bacterial cell, the poor polymerization of FtsZ84 mutant protein argues for a biological role for polymerized FtsZ. *In vivo*, a drop in FtsZ concentration to half its wild-type level virtually abolishes cell division (34). Thus, the residual polymerization of FtsZ84 is likely below that required for septum formation. That the FtsZ84 protein does retain a significant level of activity is also consistent with the observation that *ftsZ84* mutants can be rescued by increasing expression of the mutant allele (33) and also by a variety of suppressing mutations that likely alter *ftsZ* expression (33, 35, 36).

The estimated cellular abundance of FtsZ is near 0.8 mg/ml (5, 18). This is far above its critical concentration and sufficient to form at least one circumferential FtsZ tubule at the division site, consistent with a cytoskeletal role. Disassembly of FtsZ was rapid, consistent with its redistribution from the septum to the cytoplasm during the cell cycle (18).

Further evidence supporting a structural role for FtsZ, proposed by Bi and Lutkenhaus (18), is provided by the similarities between tubules formed by FtsZ and microtubules.

Localization of FtsZ. While polymerization of FtsZ occurred throughout the solution *in vitro*, it is specifically localized at the midcell membrane *in vivo*. Perhaps the location of FtsZ is regulated by a membrane protein that either nucleates polymerization or recruits the polymerized FtsZ. The septum synthesis proteins FtsH, FtsI, FtsL, FtsN, FtsQ, and FtsW all span the inner membrane (37–42). The cytoplasmic domains of one or more of these proteins may interact with FtsZ either directly or via FtsA (43, 44). The signal the cell uses to activate FtsZ assembly and how it establishes where the cell midpoint is located remain unknown.

Role and Architecture of FtsZ. At least two important structural functions can be envisaged for FtsZ protein tubules. First, FtsZ tubules at the cytoplasmic side of the inner membrane might organize the ordered synthesis of the peptidoglycan in the periplasm, as has been suggested (2), to guide FtsI and the rest of the synthetic apparatus. Simple tethering of the putative FtsI complex to FtsZ may be sufficient, restricting peptidoglycan synthesis to the midcell. Alternatively, protein motor may serve to translocate the transmembrane complex along FtsZ tubules, supplying force to overcome the resistance due to the viscosity of the inner membrane. The protofilaments of the FtsZ tubule may provide a track along which motor proteins translocate.

Second, FtsZ could also be involved in generation or transmission of the mechanical force required to overcome the outward osmotic pressure on the cell membrane. If so, FtsZ must be connected to the peptidoglycan by some transmembrane factor. This could be a second role for the FtsI complex discussed above or an additional transmembrane factor. Two mechanisms might be considered.

Boa Constrictor Model. A circumferential tubule of FtsZ polymerizes with overlapping ends. Motor proteins slide the tubule ends past each other, actively invaginating the cell wall. Several shorter tubules might overlap and each use a motor to slide along the overlapping tubule, resembling an aperture more than a boa constrictor.

Spiral Treadmill Model. As a circumferential tubule of FtsZ is polymerized, the growing end of the tubule overlaps the outer end and becomes precisely aligned in a spiral within the outer end (Fig. 6), possibly requiring a guide factor. Subunits of FtsZ depolymerize from the outer end of the tubule, while new subunits of FtsZ are added to the growing end to form a diminishing spiral. Each FtsI complex tracks toward the growing end of the tubule (counterclockwise in Fig. 6), following the same narrowing spiral as the septum is synthesized.

A single tubule may be insufficient for the required force, and the above models could easily describe the behavior of individual tubules in an array. Completion of the septum would require additional factors to cap the new cell pole, filling in the gap left by the tightest possible spiral of FtsZ. These speculations predict that FtsZ is connected to the invaginating peptidoglycan layer in a number of places by at least one type of transmembrane complex and that the tubules that encircle the cell have overlapping ends rather

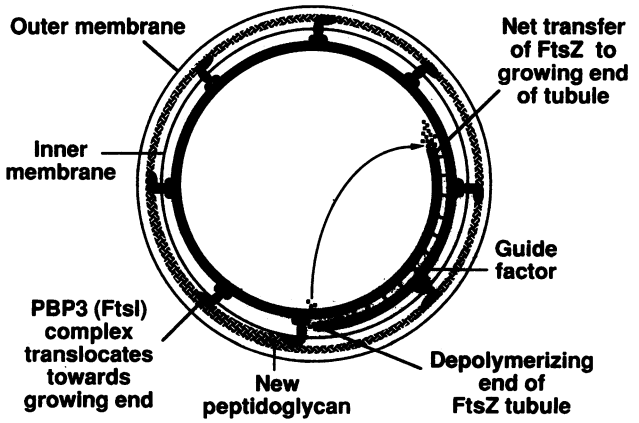

FIG. 6. Spiral treadmill model for septum synthesis. See text for details.

than being ligated into a continuous ring. Also, tubules of FtsZ should exhibit a polarity that can be recognized by at least one type of motor protein required for cell division, which translocates along FtsZ.

Comparison with Tubulin. Although homology is limited to a sequence of 7 amino acids involved in GTP binding (19, 20), like tubulin (26–28), FtsZ can polymerize to form tubules with parallel arrays of protofilaments. While determination of the exact number, arrangement, and size of FtsZ subunits in the tubules will require more detailed studies, our data allow some interesting estimates to be made. Assuming that one class of tubule is formed by FtsZ, the best fit to our data is a tubule of ≈17 nm (outer diameter) containing 12 or 13 FtsZ protofilaments of ≈3.5 nm diameter. Alternatively, several sizes of tubule may be formed, containing from 10 up to 15 FtsZ protofilaments. The FtsZ tubules are smaller than typical 25-nm microtubules, consistent with the smaller size of FtsZ (38 kDa) compared with tubulins (55 kDa) but closely similar in the number of protofilaments. Microtubules usually contain 13 protofilaments, although 12 and 14 protofilament microtubules have been observed (45).

FtsZ exhibits a critical concentration far below its cellular level, and considerably lower than that for purified tubulin. The rate of FtsZ polymerization during the initial phase exceeds that of tubulin by 100-fold or more (25). It seems likely that factors that inhibit assembly of FtsZ play an important role in regulating its cellular activity. MinCD and SulA are candidates for such factors, but others may exert cell cycle control.

The data for FtsZ polymerization also have interesting implications for tubulin biology. How does the relatively slow rate of tubulin polymerization and its high critical concentration suit it for its cellular roles?

A Bacterial Cytoskeleton. A structural role for FtsZ prompts the question of whether other bacterial cytoskeletal proteins remain to be identified, including elements for elongation and nucleoid segregation (46). However, none of these proposed structures has yet been visualized clearly in bacteria. In the absence of such evidence, a cytoskeletal role for FtsZ can only be inferred.

We thank J. Hsu for help in sequencing, R. Harrison for assistance with stopped flow measurements, M. Tota for advice and help in measuring light scattering, M. Meyenhofer for advice on preparing electron microscope samples, and Dan Bollag and Mike Rozycki for insightful discussions.

1. Nanninga, N. (1991) *Mol. Microbiol.* **5**, 791–795.
2. Lutkenhaus, J. (1993) *Mol. Microbiol.* **9**, 403–409.
3. de Boer, P. A., Cook, W. R. & Rothfield, L. I. (1990) *Annu. Rev. Genet.* **24**, 249–274.
4. Wang, X. D., de Boer, P. & Rothfield, L. I. (1991) *EMBO J.* **10**, 3363–3372.
5. Pla, J., Sanchez, M., Palacios, P., Vicente, M. & Aldea, M. (1991) *Mol. Microbiol.* **5**, 1681–1686.
6. Dai, K. & Lutkenhaus, J. (1991) *J. Bacteriol.* **173**, 3500–3506.
7. Taschner, P. E., Huls, P. G., Pas, E. & Woldringh, C. L. (1988) *J. Bacteriol.* **170**, 1533–1540.
8. Begg, K. J. & Donachie, W. D. (1985) *J. Bacteriol.* **163**, 615–622.
9. Holden, P. R., Brookfield, J. & Jones, P. (1993) *Mol. Gen. Genet.* **240**, 213–220.
10. Old, I. G., MacDougall, J., Saint-Girons, I. & Davidson, B. E. (1992) *FEMS Microbiol. Lett.* **78**, 245–250.
11. Margolin, W., Corbo, J. C. & Long, S. R. (1991) *J. Bacteriol.* **173**, 5822–5830.
12. Beall, B. & Lutkenhaus, J. (1991) *Genes Dev.* **5**, 447–455.
13. Bi, E. & Lutkenhaus, J. (1990) *J. Bacteriol.* **172**, 5602–5609.
14. Lutkenhaus, J. F. (1983) *J. Bacteriol.* **154**, 1339–1346.
15. de Boer, P., Crossley, R. E. & Rothfield, L. I. (1990) *Proc. Natl. Acad. Sci. USA* **87**, 1129–1133.
16. Bi, E. & Lutkenhaus, J. (1990) *J. Bacteriol.* **172**, 5610–5616.
17. Bi, E. & Lutkenhaus, J. (1993) *J. Bacteriol.* **175**, 1118–1125.
18. Bi, E. F. & Lutkenhaus, J. (1991) *Nature (London)* **354**, 161–164.
19. de Boer, P., Crossley, R. & Rothfield, L. (1992) *Nature (London)* **359**, 254–256.
20. Mukherjee, A., Dai, K. & Lutkenhaus, J. (1993) *Proc. Natl. Acad. Sci. USA* **90**, 1053–1057.
21. RayChaudhuri, D. & Park, J. T. (1992) *Nature (London)* **359**, 251–254.
22. Spudich, J. A. & Watt, S. (1971) *J. Biol. Chem.* **246**, 4866–4871.
23. Weisenberg, R. C. (1972) *Science* **177**, 1104–1105.
24. Shelanski, M. L., Gaskin, F. & Cantor, C. R. (1973) *Proc. Natl. Acad. Sci. USA* **70**, 765–768.
25. Gaskin, F., Cantor, C. R. & Shelanski, M. L. (1974) *J. Mol. Biol.* **89**, 737–738.
26. Amos, L. A. & Klug, A. (1974) *J. Cell Sci.* **14**, 523–550.
27. Chritien, D. & Wade, R. H. (1991) *Biol. Cell* **71**, 161–174.
28. Mandelkow, E.-M. & Mandelkow, E. (1985) *J. Mol. Biol.* **181**, 123–135.
29. Kirschner, M. & Mitchison, T. (1986) *Cell* **45**, 329–342.
30. Sandoval, I. V. & Cuatrecasas, P. (1976) *Biochem. Biophys. Res. Commun.* **68**, 169–177.
31. Sloboda, R. D., Dentler, W. L. & Rosenbaum, J. L. (1976) *Biochemistry* **15**, 4497–4505.
32. Lutkenhaus, J. F., Wolf-Watz, H. & Donachie, W. C. (1980) *J. Bacteriol.* **142**, 615–620.
33. Phoenix, P. & Drapeau, G. R. (1988) *J. Bacteriol.* **170**, 4338–4342.
34. Garrido, T., Sanchez, M., Palacios, P., Aldea, M. & Vicente, M. (1993) *EMBO J.* **12**, 3957–3965.
35. Ruberti, I., Crescenzi, F., Paolozzi, L. & Ghelardini, P. (1991) *Mol. Microbiol.* **5**, 1065–1072.
36. Gervais, F. G., Phoenix, P. & Drapeau, G. R. (1992) *J. Bacteriol.* **174**, 3964–3971.
37. Barondess, J. J., Carson, M., Guzman, L. & Beckwith, J. (1991) *Res. Microbiol.* **142**, 295–299.
38. Carson, M. J., Barondess, J. & Beckwith, J. (1991) *J. Bacteriol.* **173**, 2187–2195.
39. Guzman, L. M., Barondess, J. J. & Beckwith, J. (1992) *J. Bacteriol.* **174**, 7716–7728.
40. Tomoyasu, T., Yamanaka, K., Murata, K., Suzaki, T., Bouloc, P., Kato, A., Niki, H., Hiraga, S. & Ogura, T. (1993) *J. Bacteriol.* **175**, 1352–1357.
41. Ueki, M., Wachi, M., Jung, H. K., Ishino, F. & Matsuhashi, M. (1992) *J. Bacteriol.* **174**, 7841–7843.
42. Ikeda, M., Sato, T., Wachi, M., Jung, H. K., Ishino, F., Kobayashi, Y. & Matsuhashi, M. (1989) *J. Bacteriol.* **171**, 6375–6378.
43. Dai, K. & Lutkenhaus, J. (1992) *J. Bacteriol.* **174**, 6145–6151.
44. Dewar, S. J., Begg, K. J. & Donachie, W. D. (1992) *J. Bacteriol.* **174**, 6314–6316.
45. Dustin, P. (1984) *Microtubules* (Springer, Berlin).
46. Niki, H., Imamura, R., Kitaoka, M., Yamanaka, K., Ogura, T. & Hiraga, S. (1992) *EMBO J.* **11**, 5101–5109.